8th GRACM International Congress on Computational Mechanics
Volos, 12 July – 15 July 2015

# CESSATION OF VISCOPLASTIC POISEUILLE FLOW IN A RECTANGULAR DUCT WITH WALL SLIP

**Yiolanda Damianou, George Kaoullas, Georgios C. Georgiou**

Department of Mathematics and Statistics, University of Cyprus
P.O. Box 20537, 1678 Nicosia, Cyprus
e-mail: georgios@ucy.ac.cy ; web page: http://euclid.mas.ucy.ac.cy/~georgios

**Keywords:** Bingham Plastic; Slip; Slip Yield Stress; Poiseuille Flow; Rectangular Duct; Papanastasiou Regularization.

**Abstract.** *We solve numerically the cessation of the pressure-driven Poiseuille flow of a Bingham plastic under the assumption that slip occurs along the wall following a generalized Navier-slip law involving a non-zero slip yield stress. In order to avoid the numerical difficulties caused by their inherent discontinuities, both the constitutive and the slip equations are regularized by means of exponential (Papanastasiou-type) regularizations. As with one-dimensional Poiseuille flows, in the case of Navier slip (zero slip yield stress), the fluid slips at all times, the velocity becomes and remains plug before complete cessation, and the theoretical stopping time is infinite. The cessation of the plug flow is calculated analytically. In the case of no-slip or slip with non-zero slip yield stress, the fluid slips at the wall only in the initial stages of cessation, i.e. slip ceases at a critical time after which the flow decays exponentially and the stopping times are finite in agreement with theory. The combined effects of viscoplasticity and slip are investigated for wide ranges of the Bingham and slip numbers and results showing the evolution of the yielded and unyielded regions are presented.*

## 1 INTRODUCTION

We have recently solved numerically the steady-state Poiseuille flow of Herschel-Bulkley fluids in a duct of rectangular cross section under the assumption that slip occurs along the wall only if the wall shear stress, $\tau_w$, exceeds a critical value, $\tau_c$, known as the slip yield stress [1].

In Damianou and Georgiou [1], it has been demonstrated that there are four distinct steady-state regimes in steady Poiseuille flow in a rectangular duct, defined by three critical values of the pressure gradient. Initially no slip occurs, in the second regime slip occurs only in the middle of the wider wall, in the third regime slip occurs partially at both walls, and eventually variable slip occurs everywhere. The two intermediate partial-slip regimes collapse to one in the case of a square duct.

In order to study the combined effects of viscoplasticity and slip in this steady-state flow, Damianou and Georgiou [1] employed the Herschel-Bulkley constitutive equation. In the present work, we use the Papanastasiou regularization of the Herschlel-Bulkley equation [2], as well as a regularized form of the slip equation [3]. The latter has been tested by Damianou et al. [3] in solving the cessation of Poiseuille flow of a Herschel-Bulkley fluid in a round tube, which is one dimensional. It has also been used to solve the two-dimensional steady-state Poiseuille flow in a rectangular channel [1], giving very satisfactory results for both Newtonian and Bingham flows in those intermediate regimes where wall slip is partial, i.e. it occurs only along a part of the wall around the symmetry plane. The numerical results also agreed with the analytical solution of the Newtonian flow, in regimes where this is available (no wall slip or slip everywhere along the walls).The advantages and disadvantages of regularizations have been discussed by Balmforth et al. [4].

The objective of the present work is to investigate the effect of wall slip on the cessation flow of a Bingham plastic in a square duct. Such a time-dependent flow provides a good test for the regularizations of both the Bingham constitutive equation and the slip equation we employ. The numerical results for the cessation flow showed that in the case of Navier slip (zero slip yield stress), the fluid slips at all times, the velocity becomes and remains plug before complete cessation, and the theoretical stopping time is infinite. The cessation of the plug flow can been calculated analytically. No stagnant regions appear at the corners when Navier slip is applied. In the case of non-zero slip yield stress, the fluid may slip everywhere or partially at the wall only in the initial stages of cessation. Interestingly, numerical difficulties are osbserved in this flow regime, since the regularization becomes problematic when the rate of derormation is zero almost everywhere but not very close to the wall.

## 2 GOVERNING EQUATIONS

We consider the transient Poiseuille flow of a Bingham plastic in a duct of square cross-section and infinite length with $-H \le y \le H$, $-H \le z \le H$, where $H$ is the half-width of the duct. Due to symmetry, only the first quadrant is considered. For convenience, we work with the dimensionless equations. We scale lengths by $H$, the velocity $u$ by the mean velocity $V$ in the duct, the pressure by $\mu V/H$, where $\mu$ is the plastic viscosity, and the time $t$ by $\rho H^2/\mu$ where $\rho$ is the density. The flow is governed by the momentum equation, which, under the assumption of negligible gravity, is simplified to

$$\rho \frac{\partial u}{\partial t} = G + \nabla \cdot \boldsymbol{\tau} \tag{1}$$

where $G$ is the imposed pressure gradient and $\boldsymbol{\tau}$ is the viscous stress tensor given by the regularized Papanastasiou equation for the Bingham plastic:

$$\boldsymbol{\tau}^* = \left\{ \frac{Bn\left[1-\exp\left(-M\dot{\gamma}^*\right)\right]}{\dot{\gamma}^*} + 1 \right\} \dot{\boldsymbol{\gamma}}^* \tag{2}$$

where $\dot{\boldsymbol{\gamma}}$ is the rate of strain tensor, $\dot{\gamma}$ denotes its magnitude, and

$$Bn \equiv \frac{\tau_0 H}{\mu V} \quad \text{and} \quad M \equiv \frac{mV}{H} \tag{3}$$

are the Bingham number and the dimensionless stress growth number, respectively. The dimensionless form of the regularized slip equation is

$$\tau_w^* = B_c\left[1-\exp\left(-M_c u_w^*\right)\right] + Bu_w^* \tag{4}$$

where the slip-yield-stress number, $B_c$, the slip number, $B$, and the growth number, $M_c$, are defined as follows:

$$B_c \equiv \frac{\tau_c H}{\mu V}, \quad B \equiv \frac{\beta H}{\mu}, \quad M_c \equiv m_c V \tag{5}$$

where $\beta$ is the slip parameter, which depends on the temperature, and on the properties if the material and of the fluid/wall interface [5], $\tau_c$ is the slip yield stress and $m_c$ is a growth parameter.

## 3 ANALYTICAL SOLUTIONS FOR THE NEWTONIAN FLOW

In the case of Newtonian flow in a rectangular duct, Eq. (1) is simplified to

$$\rho \frac{\partial u}{\partial t} = G + \eta\left(\frac{\partial^2 u_x}{\partial y^2} + \frac{\partial^2 u_x}{\partial z^2}\right) \tag{6}$$

where $\eta$ is the viscosity. The steady-state solution serves as the initial condition for the cessation flow. In the case of non-zero slip yield stress there are two critical values of the pressure gradient, $G_{c1}$ and $G_{c2}$, that define three flow regimes as follows: (i) for $G \le G_{c1}$, no slip occurs (ii) for $G_{c1} < G \le G_{c2}$, slip occurs in the middle of the edges but not near the corners and the problem is not amenable to analytical solution; (iii) for $G > G_{c2}$, non-uniform slip occurs everywhere. We scale the velocity by $H\tau_c/\eta$, the pressure gradient by $\tau_c/H$, $y$ and $z$ by $H$, and time by $H^2/\nu$. The non-dimensionalized values of the critical pressure gradients are

$$G_{c1}^* = \frac{1}{4\sum_{i=1}^{\infty}\sum_{j=1}^{\infty}\frac{(-1)^{j+1}}{\alpha_{i,j}^2\alpha_j}} \tag{7}$$

and

$$G_{c2}^{*}=\frac{1}{4\sum_{i=1}^{\infty}\sum_{j=1}^{\infty}\frac{A_{i,j}\lambda_i\sin\lambda_i\cos\lambda_j}{\lambda_{i,j}^{2}}} \tag{8}$$

where

$$\alpha_i\equiv(2i-1)\pi/2 \quad \text{and} \quad \alpha_{i,j}^{2}\equiv\alpha_i^{2}+\alpha_j^{2},\quad i,j=1,2,\cdots \tag{9}$$

$$\lambda_i\tan\lambda_i=B \quad \text{and} \quad \lambda_{i,j}^{2}\equiv\lambda_i^{2}+\lambda_j^{2},\quad i,j=1,2,\cdots \tag{10}$$

and $B\equiv\beta H/\eta$ is the slip number. Moreover,

$$A_{i,j}\equiv\frac{\sin(\lambda_i)\sin(\lambda_j)}{\lambda_i\lambda_j\left(1+\sin^{2}(\lambda_i)/B\right)\left(1+\sin^{2}(\lambda_j)/B\right)} \tag{11}$$

The velocity and volumetric flow rate can then be written as follows:

$$u_x^{*}\left(y^{*},z^{*},t^{*}\right)=\begin{cases}4G^{*}\sum_{i=1}^{\infty}\sum_{j=1}^{\infty}\frac{(-1)^{i+j}}{\alpha_{i,j}^{2}\alpha_i\alpha_j}\cos\left(\alpha_i y^{*}\right)\cos\left(\alpha_j z^{*}\right)\exp(-\alpha_{i,j}^{2}t^{*}), & G^{*}\le G_{c1}^{*}\\ 4G^{*}\sum_{i=1}^{\infty}\sum_{j=1}^{\infty}A_{i,j}\frac{1}{\lambda_{i,j}^{2}}\cos\left(\lambda_i y^{*}\right)\cos\left(\lambda_j z^{*}\right)\exp(-\lambda_{i,j}^{2}t^{*})-\frac{1}{B}, & G^{*}\ge G_{c2}^{*}\end{cases} \tag{12}$$

and

$$Q^{*}(t^{*})=\begin{cases}4G^{*}\sum_{i=1}^{\infty}\sum_{j=1}^{\infty}\frac{1}{\alpha_{i,j}^{2}\alpha_i^{2}\alpha_j^{2}}\exp(-\alpha_{i,j}^{2}t^{*}) & G^{*}\le G_{c1}^{*}\\ 4G^{*}\sum_{i=1}^{\infty}\sum_{j=1}^{\infty}A_{i,j}\frac{\sin(\lambda_i)\sin(\lambda_j)}{\lambda_{i,j}^{2}\lambda_i\lambda_j}\exp(-\lambda_{i,j}^{2}t^{*})-\frac{1}{B}, & G^{*}\ge G_{c2}^{*}\end{cases} \tag{13}$$

In the two expressions above, the solution for $G^{*}\le G_{c1}^{*}$ holds at all times, while the solution for $G^{*}>G_{c2}^{*}$ holds only up to the critical time $t_c^{*}$ at which slip at the duct corner ceases. The time $t_c^{*}$ is the root of the following equation:

$$\sum_{i=1}^{\infty}\sum_{j=1}^{\infty}A_{i,j}\frac{1}{\lambda_{i,j}^{2}}\cos\lambda_i\cos\lambda_j\exp(-\lambda_{i,j}^{2}t_c^{*})=\frac{1}{4BG^{*}} \tag{14}$$

## 4 NUMERICAL RESULTS ON CESSATION OF NEWTONIAN FLOW

All the results of this section have been obtained with a 100×100-biquadratic finite element mesh and $M=10^{6}$. A fully-implicit scheme has been used for the time integration. The analytical solutions for the Newtonian flow for the no-slip, the Navier-slip, and the non-zero slip yield stress cases served as good tests for the numerical code and the regularized slip equation.

The steady-state flow curve, i.e. the plot of the volumetric flow rate versus the imposed pressure gradient, for $B=1$ is shown in Fig. 1. Three flow regimes are defined by the two critical values $G_{c1}^{*}=1.4808$ and $G_{c2}^{*}=2.6290$: (a) for $G^{*}\le G_{c1}^{*}$, there is no slip along the duct walls; (b) for $G_{c1}^{*}<G^{*}\le G_{c2}^{*}$ slip is partial, i.e. it

occurs in the middle of each edge and not close the corners; and (c) for $G^* > G^*_{c2}$ slip occurs everywhere along the boundary. The velocity contours for three representative values of the pressure gradient, i.e. $G^*$=1, 2, and 3, corresponding to the three regimes are also illustrated in Fig. 1.

In Fig. 2, we plotted the evolution of the maximum velocity ($u^*_{\max}$), the maximum slip velocity at the middle of the edges ($u^*_{w,\max}$), and the minimum slip velocity at the corners ($u^*_{w,\min}$). It is shown that $u^*_{w,\min}$ vanishes at $t^*_{c1} = 0.0674$. Beyond that time, slip at the wall is partial till the critical time $t^*_{c2} = 0.3503$ at which slip ceases and $u^*_{w,\max}$ vanishes.

## 5 NUMERICAL RESULTS ON CESSATION OF BINGHAM PLASTIC FLOW

In order to determine accurately the yielded and unyielded regions with a regularization method, one needs to employ fine meshes and a rather high value of the regularization parameter. This was also emphasized in our previous work on the steady-state flow [1]. As in the previous section, we used a $100\times100$-element mesh with $M = 10^6$. The "unyielded" areas have been determined as the areas where $\tau^* \le Bn$ (von Mises criterion).

In general, time-dependent Bingham flows require smaller time-steps than their Newtonian counterparts. In the beginning of the cessation flow, we found it necessary to reduce the time step down to 0.001 times its nominal value $\Delta t^*$ and gradually increase it up to its nominal value at $t^* = \Delta t^*$. Another observation we made was that coarser meshes require even smaller time steps in order to avoid divergence.

### 5.1 No wall slip

Results have been obtained when the volumetric rate is imposed initially ($Q$=1) and the corresponding pressure gradient (which depends on the Bingham number) is suddenly set to zero. In Figs. 3 and 4, the results for $Bn$=0.1 and 10 are presented. Obviously, the stopping time is reduced as the Bingham number is increased. The numerical stopping times, i.e. the times at which $Q$ becomes $10^{-3}$ were found to be equal to 0.674 and 0.0483 for $Bn$=0.1 and 10, respectively. These agree very well with the theoretical estimates of Glowinski [6].

It should be noted that using a very refined mesh may lead to convergence difficulties in the final stages of cessation, i.e. when the velocity is close to zero and thus flat. In such a case the magnitude of the rate-of-strain tesnor is almost zero and thus the use of the regularized constitutive equation becomes problematic. It seems that the main advantage of a fine mesh is the possibility of drawing more accurate and smoother yielded regions for times very close to complete cessation. But if convergence becomes difficult then the only other option is to reduce $M$, which again leads to inaccurate unyielded regions.

### 5.2 Navier slip

In order to visualize the combined effects of slip and viscoplasticity during cessation, we consider once again the evolution of the maximum velocity at the duct center ($u_{\max}$), the maximum slip velocity at the middle of the wall ($u_{w,\max}$), and the minimum slip velocity at the duct corner ($u_{w,\min}$). Obviously, in the absence of slip, $u_{w,\max} = u_{w,\min} = 0$. Moreover, if the growing inner unyielded core reaches the wall, then $u_{w,\max} = u_{\max}$ and if $u_{w,\min} = u_{\max}$, then the velocity is plug.

When the Navier-slip boundary condition is applied, the slip number $B$ in Newtonian flow can take any value from zero (full slip) to infinity (no-slip). In Bingham plastic flow, however, full-slip (i.e. plug flow) is attained at a finite value of $B$, which turns out to be $B_{crit} = Bn/\sqrt{2}$ for a square duct [1]. The evolution of the above quantities along with the unyielded regions and velocity contours for $Bn$=10 and various slip numbers in the range $(B_{crit}, \infty)$ is illustrated in Figs. 5 and 6. Figure 5 shows results for the no-slip case ($B = \infty$). The maximum and minimum slip velocities are of course zero and, as expected, $u_{\max}$ is always higher than $Q$; the two curves intersect only when the flow ceases, i.e., when both quantities vanish.

The results of Fig. 6 for $B$=20 correspond to strong slip. As the fluid decelerates, the central plug region grows and reaches the wall. As a result, the curves of $u_{w,\max}$ and $u_{\max}$ merge. The minimum slip velocity $u_{w,\min}$

initially decays slowly and then remains practically constant till the velocity becomes plug. Once it touches the wall, the plug zone continues growing towards the corner and the yielded region becomes triangular in shape while the velocity contours are straight lines.

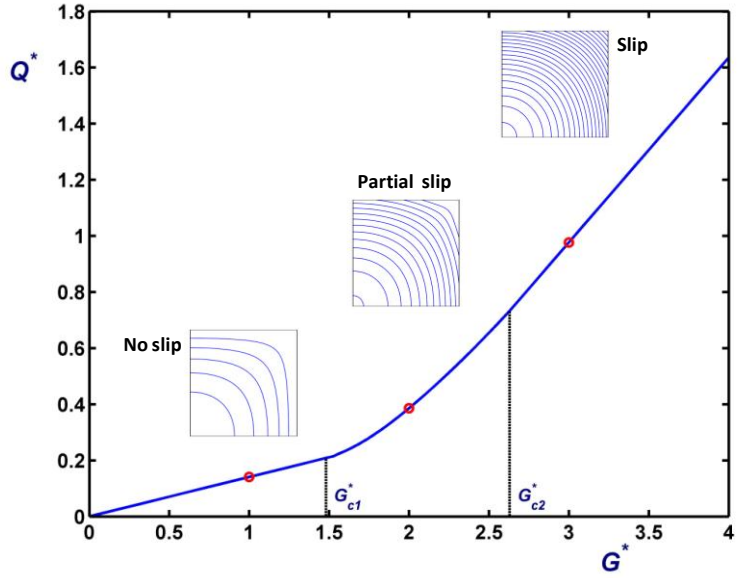


Figure 1. Flow curve of Newtonian Poiseuille flow in a square duct in the case of non-zero slip yield stress with $B$=1. Three flow regimes are defined by the two critical values of the imposed pressure gradient ( $G_{c1}^{*} = 1.4808$ and $G_{c2}^{*} = 2.6290$ ). The velocity contours for three representative values of the pressure gradient in the three flow regimes ($G^{*}$=1, 2, and 3) are also shown.

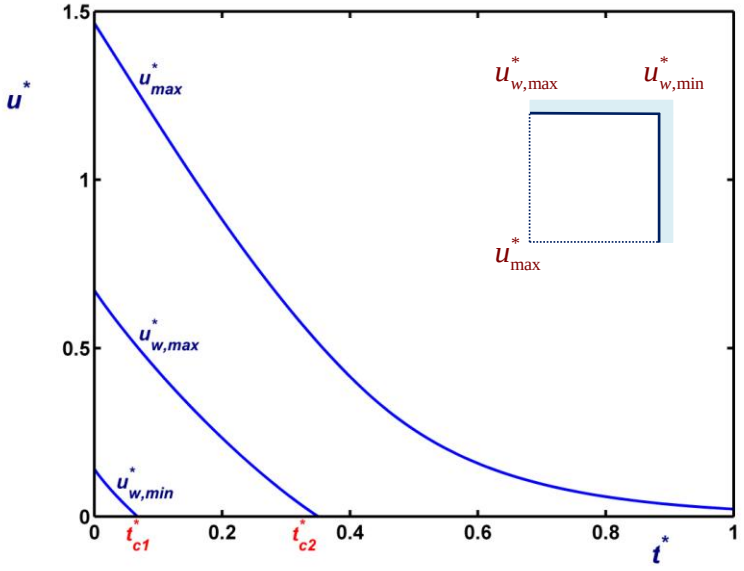


Figure 2. Evolution of the maximum velocity at the duct center, the maximum slip velocity at the middle of the duct wall, and the minimum velocity at the corners during cessation of Newtonian flow in the case of non-zero slip yield stress with $B$=1 and $G^{*} = 3 > G_{c2}^{*}$ (slip occurs everywhere at $t^{*} = 0$ ).

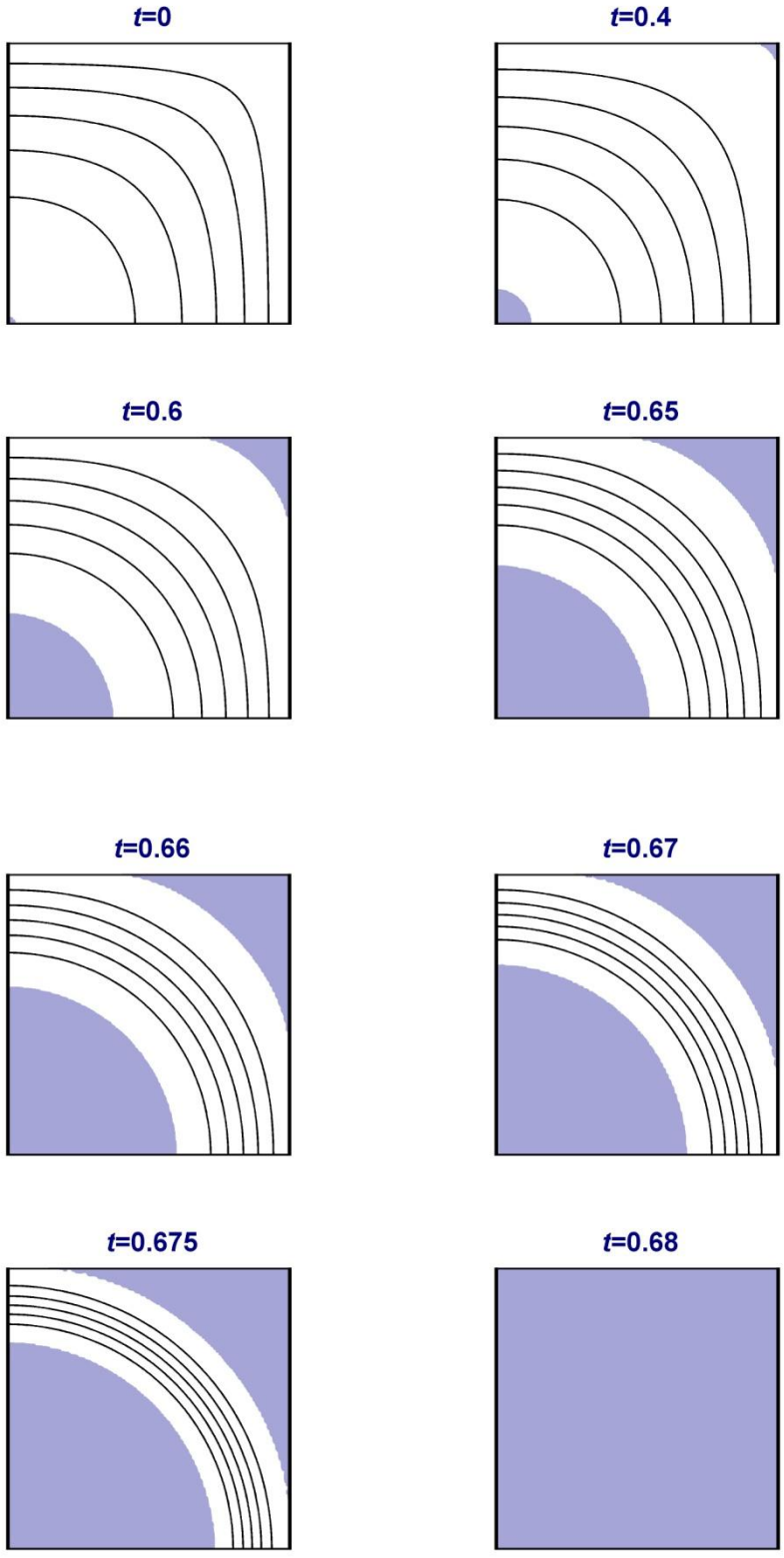


Figure 3. Unyielded areas (shaded) and velocity contours in cessation of Bingham flow in a square duct with no slip at the wall for $Bn$=0.1.

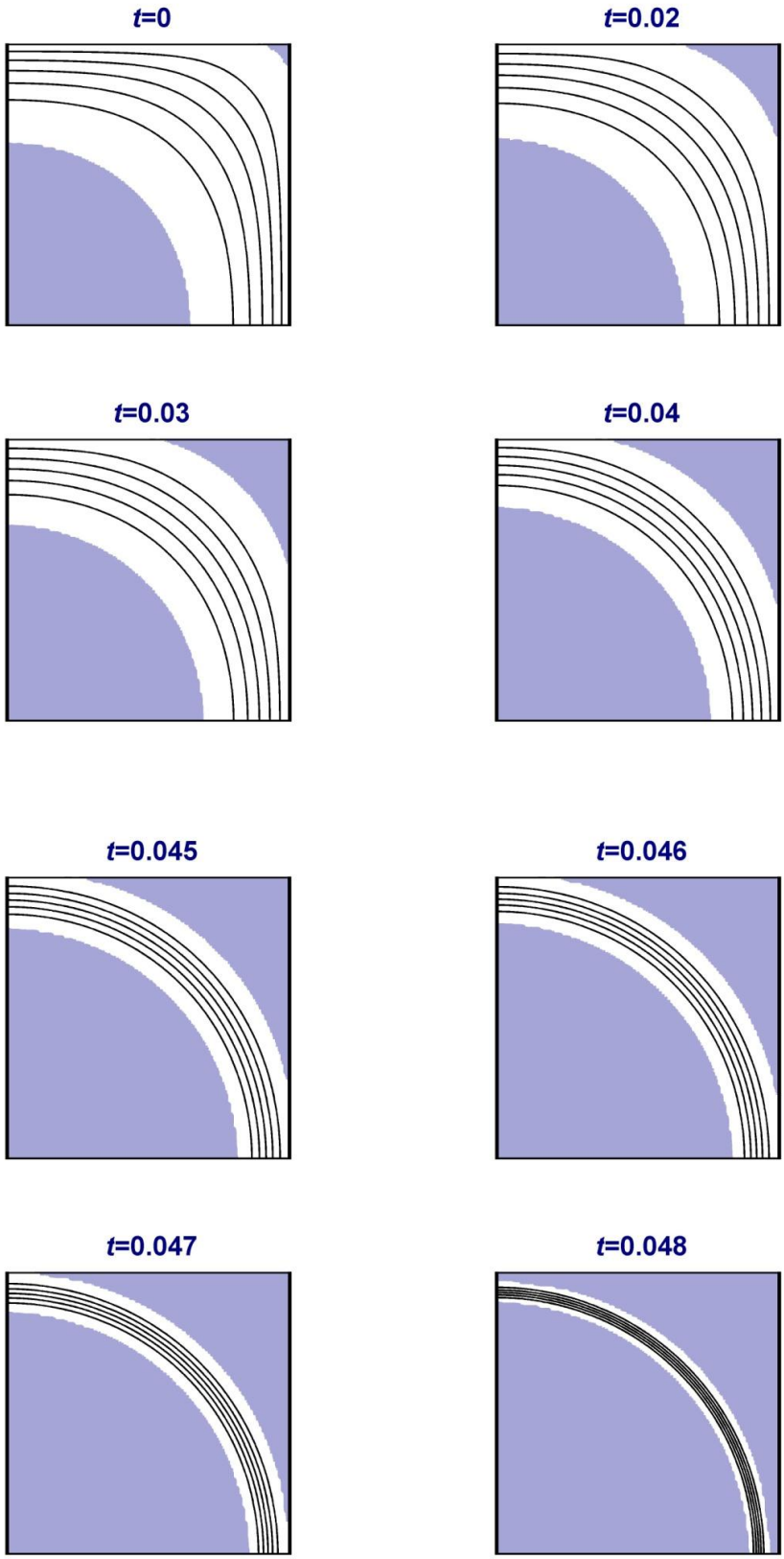


Figure 4. Unyielded areas (shaded) and velocity contours in cessation of Bingham flow in a square duct with no slip at the wall for $Bn$=10.

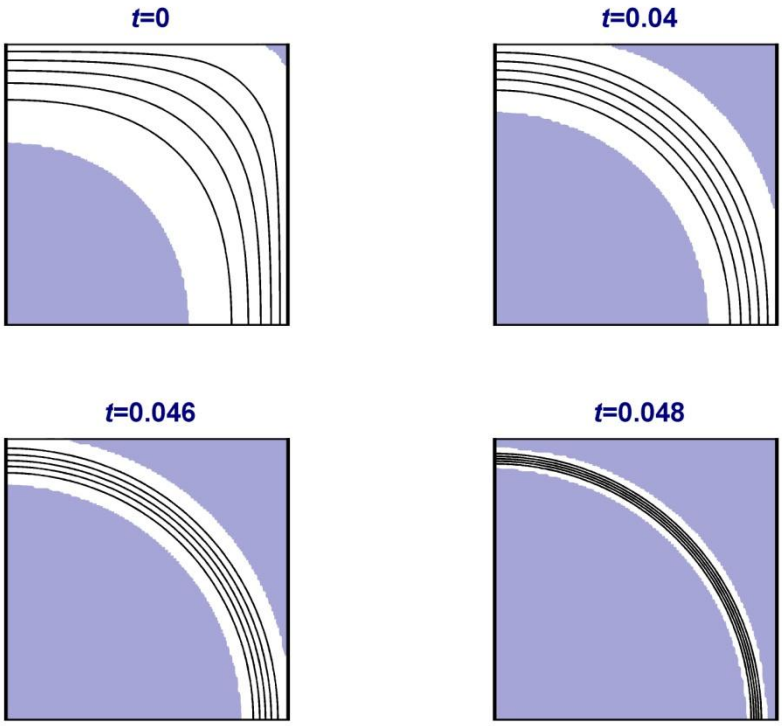


**(a)**

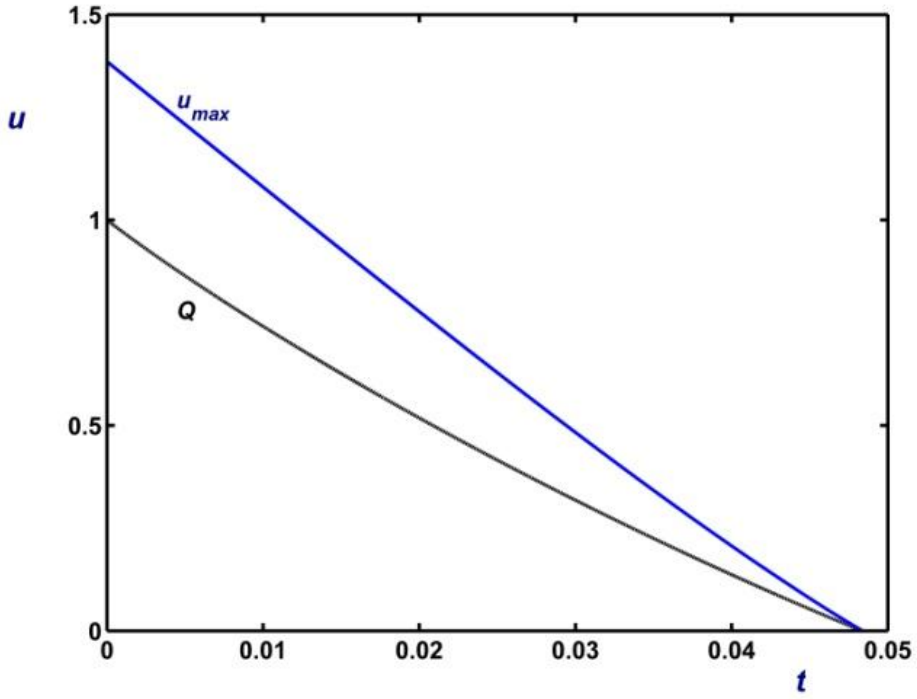


**(b)**

Figure 5. Cessation of Bingham flow in a square duct with no slip at the wall for $Bn$=10: (a) Unyielded areas (shaded) and velocity contours; (b) Evolution of the volumetric flow rate ($Q$) and the maximum velocity at the duct center ($u_{max}$).

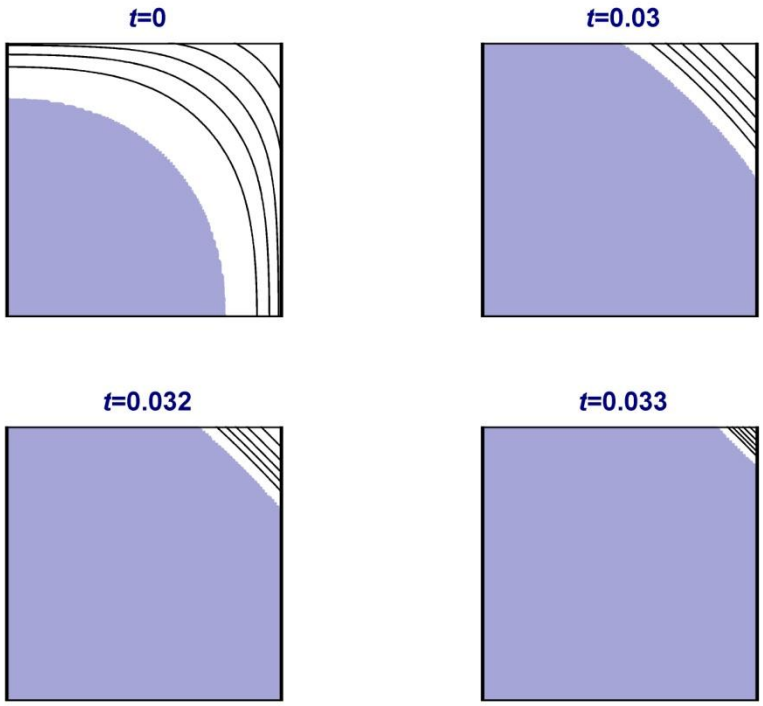


**(a)**

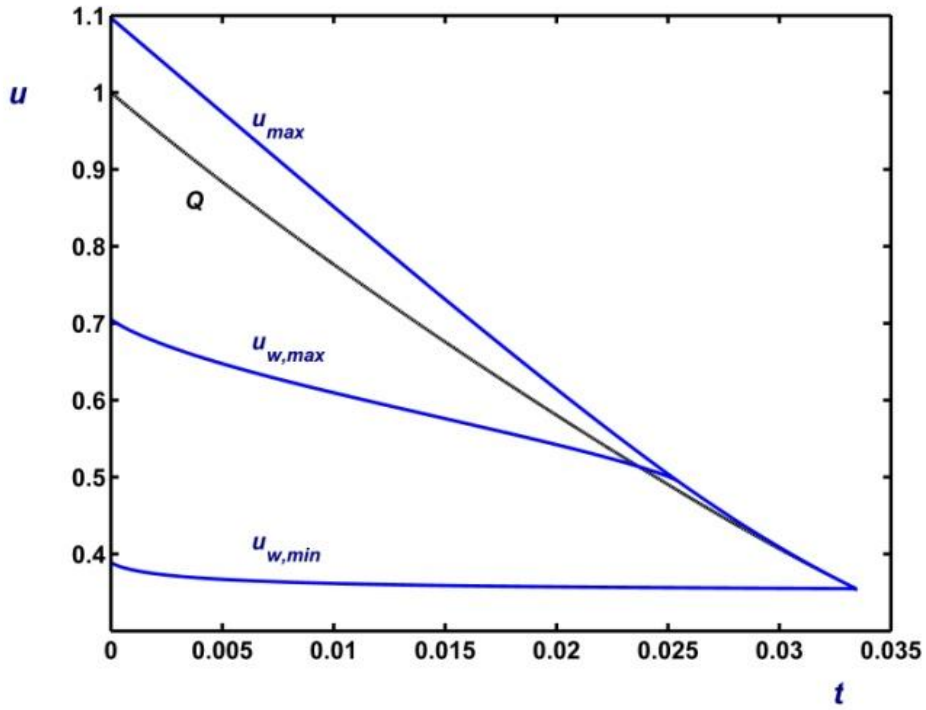


**(b)**

Figure 6. Cessation of Bingham flow in a square duct with wall slip for $Bn$=10 $B$=20: (a) Unyielded areas (shaded) and velocity contours; (b) Evolution of the volumetric flow rate ($Q$), the maximum velocity at the duct center ($u_{max}$), the maximum slip velocity at the middle of the duct walls ($u_{w,max}$), and the minimum slip velocity at the duct corners ($u_{w,min}$).

## 6 CONCLUSIONS

We solved numerically the cessation of Bingham-plastic Poiseuille flow in a square duct with wall slip and non-zero slip yield stress using regularized versions of both the constitutive and the slip equations. The analytical solutions for the Newtonian flow have been provided for the non-zero slip yield stress cases. These served as good tests for the numerical code and the regularized slip equation.

The combined effects of viscoplasticity and slip have been investigated and the evolution of the unyielded regions has been studied. In the case of no-slip, the unyielded plug core and the corner stagamt zones grow during cessation and merge inside the duct causing the flow to stop at a finite time. The numerical stopping times are in excellent agreement with the theoretical estimates of Glowinski [6]. It has been demonstrated that when Navier slip is applied there are no stagnant regions near the duct corners. The plug core grows during cessation reaching the wall and continues growing towards the corners and the shrinking yielded corner region acquires the shape of an equilateral orthogonal triangle. Eventually the velocity becomes flat at a finite time before complete cessation. A simple analytical expression describes the decay of the flat velocity. This is exponential and thus the theoretical stopping time is infinite.

We are currently investigating the case of slip with non-zero slip yield stress.

## REFERENCES

[1] Damianou, Y. and Georgiou, G.C. (2014), "Viscoplastic Poiseuille flow in a rectangular duct with wall slip", *Journal of non-Newtonian Fluid Mechanics*, Vol. 214, pp. 88-105.

[2] Papanastasiou, T.C. (1987), "Flows of materials with yield", *Journal of Rheology*, Vol. 31, pp. 385.

[3] Damianou, Y., Philippou, M. Kaoullas, G. and Georgiou, G.C. (2014), "Cessation of viscoplastic Poiseuille flow with wall slip", *Journal of non-Newtonian Fluid Mechanics*, Vol. 203, pp. 24-37.

[4] Balmforth, N.J., Frigaard, I.A. and Ovarlez, G. (2014), "Yielding to stress: Recent developments in viscoplastic fluid mechanics", *Annual Review of Fluid Mechanics*, Vol. 46, pp. 121-46.

[5] Denn, M.M. (2001), "Extrusion instabilities and wall slip", *Annual Review of Fluid Mechanics*, Vol. 33, pp. 265-287.

[6] Glowinski, R. (1984), *Numerical Methods for Nonlinear Variational Problems*, Springer-Verlag, New York